

Simulation and evaluation of a straight-bladed Darrieus-type cross flow marine turbine

S Lain* and C Osorio

Energetics and Mechanics Department, Fluid Mechanics Research Group, Universidad Autónoma de Occidente, Cali (Colombia)

Received 04 August 2010; revised 07 October 2010; accepted 12 October 2010

This study presents numerical simulations of a cross-flow vertical-axis marine current turbine (straight-bladed Darrieus type) with particular emphasis on rotor-performance prediction and hydrodynamic characteristics. Numerical investigations of a model turbine (power coefficient and flow behaviour) were undertaken using developed computational models. Turbine design was studied using a time-accurate Reynolds-averaged Navier–Stokes (RANS) commercial solver (Fluent v. 6.3). A physical transient-rotor-stator model with a sliding mesh technique was used to capture change in flow field at a particular time step. A shear stress-transport $k\text{-}\epsilon$ turbulence model was used to model turbulent features of the flow. Developed model can effectively predict hydrodynamic performance of a vertical-axis marine current turbine.

Keywords: Hydrodynamics, Numerical simulation Turbulence model, Vertical axis water turbine

Introduction

Water turbines can be classified depending on the direction of rotational axis relative to water flow direction. Axial flow water turbines (AFWT) have their axis of rotation parallel to water stream direction. Other turbines [cross flow water turbines (CFWT) or Darrieus type water turbines (from Jean-Marie Darrieus, inventor of first vertical axis wind turbine, VAWT)] have rotational axis perpendicular to current direction. A vertical-axis turbine is able to extract power from any direction without adjustment.

Based on computational tools available, different models developed range from computationally inexpensive but low in accuracy momentum models, to three-dimensional computational fluid dynamics (CFD) models of turbine. There are two families of potential flow codes and CFD codes to numerically model a tidal turbine. With the use of powerful computers and parallel processing technology, CFD simulations are becoming more popular in industrial and academic sectors¹⁻³. Contrary to potential flow codes, CFD simulations do not need any external data (experimental lift and drag) and can include separation from foils and drag induced vortices from turbine's shaft. CFD modelling is also a powerful tool for

complex geometries. However, CFD simulations for tidal turbines still suffer from high computational cost and time. Main advantage of CFD is that it allows reproducing physical unsteady flow around turbine using sliding mesh methodology, wherein relative motion between steady domain and rotor (unsteady domain) is captured by coupling them through an interface, which is updated at each time step and allows conservative interchange of fluxes between both domains. Rotor grid turns at each time step an angle relative to steady domain. At each time step a new solution is calculated. Transient behaviour is built by adding solutions at each time step. In this methodology, integral values (torque) must be averaged in a complete revolution. Disadvantage of CFD is huge need of CPU time and memory.

Ferreira⁴, employing air as fluid, presented a detailed state of art of different strategies for predicting aerodynamic characteristics of a VAWT. Also using air as fluid, Maître *et al*⁵ applied sliding mesh strategy to a two bladed VAWT using Fluent v. 6.0 software combined with the one equation turbulence model Spalart-Allmaras. Using water as fluid, Nabavi⁶ performed a very detailed numerical study about hydrodynamic performance of a three-bladed CFWT introduced in a duct, to accelerate flow upstream the turbine. This result is in line with that obtained by Maître *et al*⁵ because both used Spalart-Allmaras turbulence model. Dai & Lam⁷ performed

* Author for correspondence

E-mail: santiago.lain@gmail.com, slain@uao.edu.co

numerical study of a three-bladed CFWT using software ANSYS CFX v. 11. In this case, turbulence model chosen was two equation model SST (Shear Stress Transport). In this case, enough information was provided on geometric parameters of turbine, so this configuration has been chosen in present work.

This study performs simulation of flow around a CFWT using CFD tools, including underlying turbulence of fluid flow and also viscous effects, without employing tabulated lift and drag data.

Experimental Section

Vertical Axis Turbine Operation

Hydraulic operation of a water turbine can be characterized by rotor torque M , rotor drag D , rotor angular velocity $\dot{\omega}$ and power output $P = \dot{\omega} M$. These values can be made dimensionless as

$$\text{Tip speed ratio (TSR), } \lambda = \omega R / V_0 \quad \dots(1)$$

$$\text{Torque coefficient, } C_m = M / \left(\frac{1}{2} \rho V_0^2 R S_{ref} \right) \quad \dots(2)$$

Power coefficient or efficiency,

$$C_p = P / \left(\frac{1}{2} \rho V_0^3 S_{ref} \right) \quad \dots(3)$$

$$\text{Drag coefficient, } C_D = D / \left(\frac{1}{2} \rho V_0^2 S_{ref} \right) \quad \dots(4)$$

With R being maximum radius of rotor, V_0 incident current velocity, ρ water density and S_{ref} cross section ($S_{ref} = \pi R^2$ for AFWT and $S_{ref} = 2RH$ for CFWT). Solidity is defined as $\sigma = NC/R$ with N number of blades and C chord length. H is blade span.

Turbine blades rotate around vertical axis with rotation vector $\vec{\omega}$. In 2D cylindrical coordinates (r, θ), blade local relative velocity \vec{W} corresponding to an incident flow velocity \vec{V}_0 , is given as

$$\vec{W} = \vec{V}_0 - \vec{\omega} \times \vec{R} \quad \dots(7)$$

When a blade rotates, its angle of attack α (an angle between local relative velocity and chord) changes leading to variable hydrodynamic forces as

$$\alpha = \tan^{-1} \left(\frac{\sin \theta}{\lambda + \cos \theta} \right) \quad \dots(8)$$

Resultant hydrodynamic force acting on airfoils is decomposed in two components (normal F_n , perpendicular to chord; and tangential F_t , parallel to chord). Forces values can be inferred from classical computations over an airfoil in an unbounded domain or from available experiments in wind tunnel tests at fixed α and Reynolds number. In upstream semi circle, with θ increasing from 0° position, tangential force becomes positive and reaches a maximum near $\theta = 90^\circ$ before decreasing until $\theta = 180^\circ$. Same behaviour occurs in downstream semicircle between $\theta = 180^\circ$ and 360° positions. Positive tangential component is responsible for turbine rotation. In vicinity of $\theta = 0^\circ$ and 180° positions, blade has a negative tangential component force F_t , opposed to rotational motion. In this configuration of blades, small tip speed ratios lead to large incidence variations during a revolution. In particular, α becomes very large and overtakes static stall angle of foils, about $12-15^\circ$.

Real flows around blades in CFWT may differ from above conclusions because of two points: i) Relative flow passing through a CFWT blade is unsteady; and ii) Oncoming far field seen by a blade is not V_0 , but some unspecified velocity. Flow field around a Darrieus type CFWT is inherently unsteady and three-dimensional due to dynamic stall phenomenon experienced by a rotating blade and also to interference of detached vortices from moving blades⁸. Such vortices stay near generating blade. Therefore, a strong coupling between them and flow around blade increases lift, improving turbine efficiency. These mechanisms of vortex detachment are similar to those observed in helicopter rotors.

Geometric Configuration and Mesh Generation

CFWT⁴ has been chosen in this study due to availability of all geometric data (radius, 450 mm; reference area $S_{ref} = 0.63 \text{ m}^2$) of a turbine. Span of straight blades (700 mm) are based on symmetric NACA0025 airfoil. Considered case has been 3S2R1⁷ (profile chord, 132.75 mm), resulting in a solidity $\sigma = 0.89$. Geometry employed in simulation is a two-dimensional version of real three-dimensional turbine. Moreover, neither supporting arms of blades nor shaft have been included⁷. Dimensions (length, 8 rotor diam; width, 5 rotor diam) of simulation domain³ result in a blockage ratio (20%).

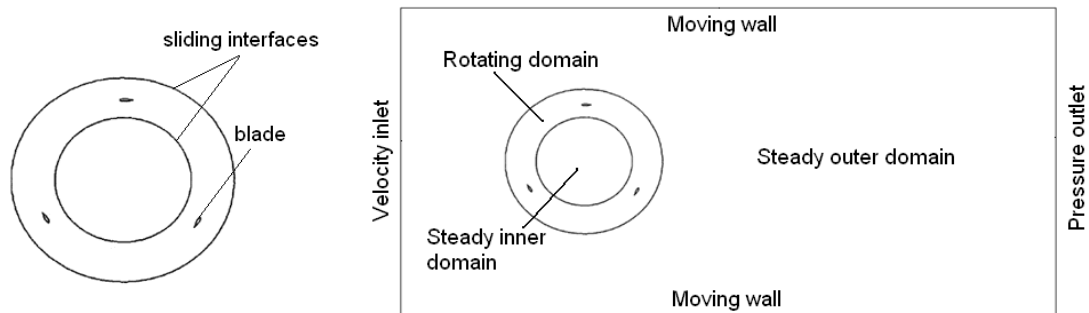


Fig. 1—Geometry of three-bladed CFWT of Dai & Lam⁴

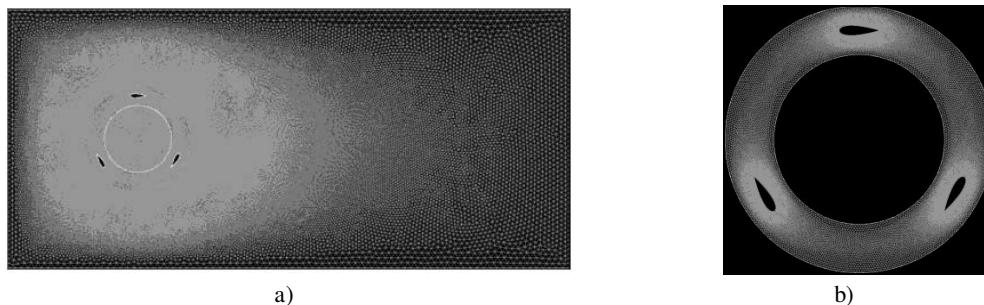


Fig. 2— a) Details of generated grid; b) detail of the grid in rotating ring containing profiles

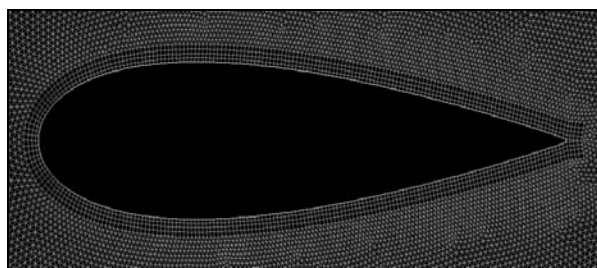


Fig. 3—Detail of grid near profile surface showing prism layer

Boundary conditions employed in two-dimensional computations (Fig. 1) consist of a velocity inlet on left side, a pressure outlet on right and two moving walls on top and bottom with same fluid velocity as inlet. Profiles representing blades are in inner part of a rotating ring, which is separated from two steady domains (inner and outer) by two sliding interfaces specified as a boundary condition of type sliding mesh. In case of CFWT, computational domain consists of a rotating zone (rotor in a ring-like domain) and a steady zone, which includes water environment outside and inside of ring-like domain (Fig. 2). Mesh closest to profiles must be refined to describe with sufficient precision the boundary layer flow. Created mesh had an O-grid topology based on quads (Fig. 3). Outside of this prism layer, a non-structured

grid based on triangles was chosen, keeping an aspect ratio similar to that of quads⁹.

Steady domain was also discretised with a non-structured grid based on triangles (Fig. 2). Grid node density is higher near blades than in rest of the domain. Moreover, due to complexity of flow in turbine wake, also grid node density is higher downstream than upstream CFWT. Most interesting zone for simulation is ring-like domain, where flow interacts with blades, which is responsible for turbine performance. Again, in this region, grid node density is higher than in steady domain.

Results and Discussion

Verification

Verification process of CFD simulation implies to perform calculation in different grids varying number of nodes, for evaluating convergence of most relevant variables, which in this case has been torque transferred from fluid to blades. Grid node densities were: coarse, 60,558; medium, 157,130; and fine, 297,302. A grid that represents a compromise between precision and computational cost was selected. Results of validation in three different grids for average torque coefficient were: coarse, 0.1200; medium, 0.1399; and fine, 0.14352. Along a complete revolution of blades ($\lambda = 1.745$), C_m obtained

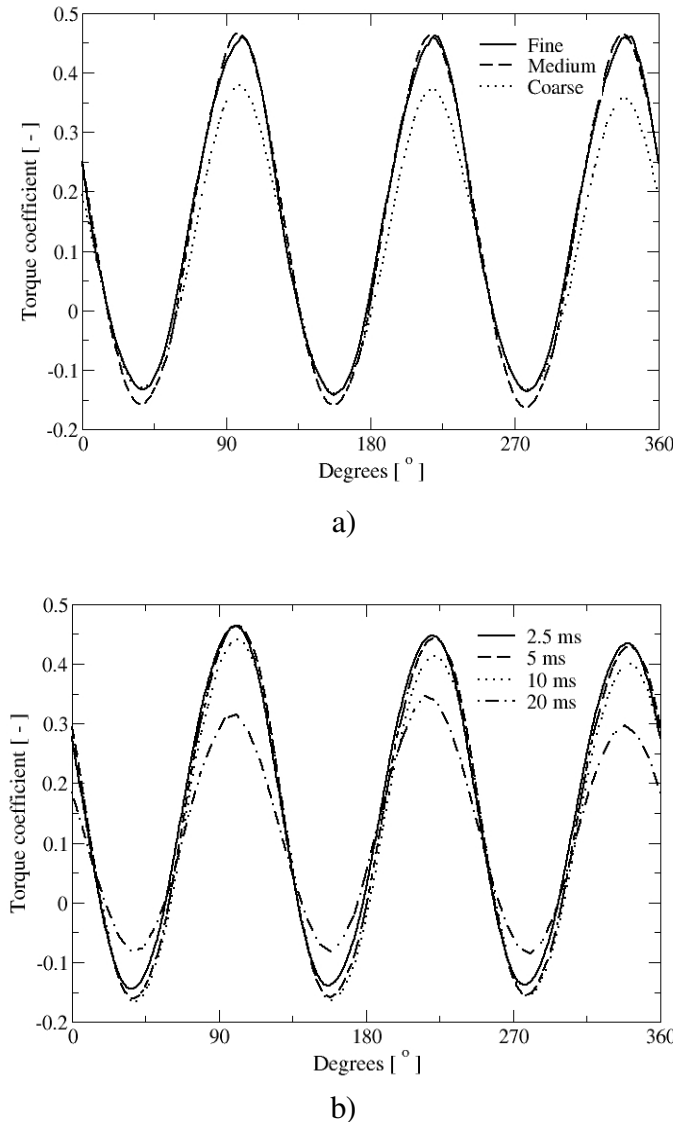


Fig. 4—Torque coefficient at $\lambda = 1.745$ for: a) Grid convergence; and b) Different time steps in medium grid

for three grids (Fig. 4a) and C_m obtained with different time steps for medium grid (Fig. 4b) are presented.

Simulation Set-up

Numerical simulations of straight-bladed CFWT were carried out using software Fluent v. 6.3, based on finite volume method. Due to symmetrical characteristics of turbine, all computations were performed by assuming a two-dimensional incompressible turbulent flow to reduce demands on computational resources. In unsteady simulation, a transient rotor stator model was employed to capture change of flow field at a particular time. A moving mesh technique was applied to rotate turbine blades at a constant rotational speed. Shear stress transport (SST) $k-\omega$ turbulence model, a combination of $k-\epsilon$ and

$k-\omega$ models¹⁰, was used to model turbulent features of flow. SST $k-\omega$ model gives superior results for flows with strong adverse pressure gradients such as those appearing in CFWT flow configuration.

Effectiveness of physical transport within Fluent v. 6.3 solver depends not only on turbulence model but also on discretisation scheme. Diffusive term in equations is discretised using second order centered differences as usual. However, for advection term, a second order upwind scheme is utilized. Pressure-velocity coupling algorithm chosen has been transient SIMPLE. Finally, time integration is performed by a second order implicit scheme to obtain a good resolution in time.

Typically, simulation starts with computation of steady flow around a fixed position of turbine blades. From this initial condition, transient simulation begins, firstly with first order schemes to ease convergence. Once that total torque on turbine has reached a quasi-periodic regime, after 3 or 4 complete rotor revolutions, discretisation schemes are switched to second order. Finally, simulation runs during a sufficient number of rotor revolutions in quasi-periodic regime to extract an average value for torque, which is used to estimate turbine performance.

Results

Average torque estimated for $\lambda = 1.745$ in present work (medium size grid and $\Delta t = 5$ ms) are found closer to experiments by Dai & Lam⁴ with CFX and double multiple streamtube model (DMS) in experimental case 3S2R1 (Table 1). In present work, C_m and C_p have been calculated according to Eqs (2) and (3), whereas in Dai & Lam⁴ work, total torque is addition of three blade torques and multiplication by a factor to take into account height difference between physical prototype and that of computational model. This is why, in present work, C_m is slightly above but C_p below that of Dai & Lam⁷ work. Flow field around turbine is quite complex because, as blades rotate, high and low velocity zones appear, leading to a detachment of boundary layer in certain angular positions. However, flow behind CFWT has low velocities, implying a smaller contribution to total torque than in upstream region.

At $\lambda = 1.745$ and $\Delta t = 5$ ms, C_m total (Fig. 5a) and C_m for each blade (Fig. 5b) are presented. In this case, real time of simulation was 14 s and 2800 time steps, equivalent to 14 complete revolutions. CPU time necessary was around 64 h. Altering time by 6 s (Fig. 5a), C_m reached a quasi-periodic regime after initial

Table 1—Comparison of results of Dai & Lam⁴ and present work

Specifications at $\lambda = 1.745$	Dai & Lam ⁴		Present study	
	Simulation CFX	DMS Model	Experiments	Simulation FLUENT
C_m , Nm	58.6	46.3	52.0	52.8
C_p , %	27.5	21.5	26.5	24.8

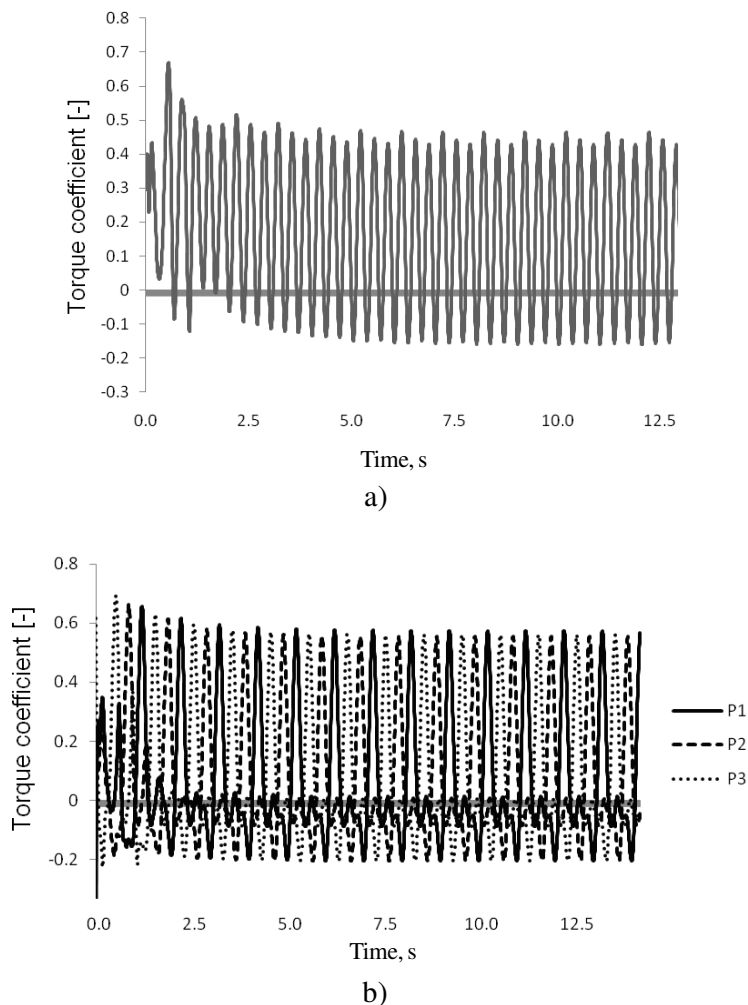


Fig. 5—Torque coefficient versus time: a) Total; and b) Each blade

transient. Both maxima and minima of C_m by each blade (Fig. 5b) have higher absolute value than total C_m due to existence of cancellations and compensations of torque among blades, resulting in a total C_m lower than that experienced by a single blade. In a turn, each blade produces a positive C_m in about a third of revolution, whereas in other two thirds, C_m is slightly negative. After averaging three coefficients generated by blades, a nearly sinusoidal curve is obtained with three positive maxima at each turn (Fig. 6) and three negative minima, meaning that during a revolution there are periods of time where

turbine produces torque on fluid. Number of maxima at each turn equals number of blades of turbine.

Plot of average C_m versus λ (Fig. 7a) shows positive values of λ close to 2.1, meaning that fluid is providing torque to turbine. Beyond $\lambda = 2.1$, C_m is negative, indicating that turbine, rotating at constant angular speed, exerts torque on the fluid. This is because a high λ implies a high turbine angular speed and, in such case, kinetic energy contained in flow is not enough to deliver torque to CFWT and make it to rotate with same angular velocity. On the other hand, curve $C_m(\lambda)$ presents a maximum

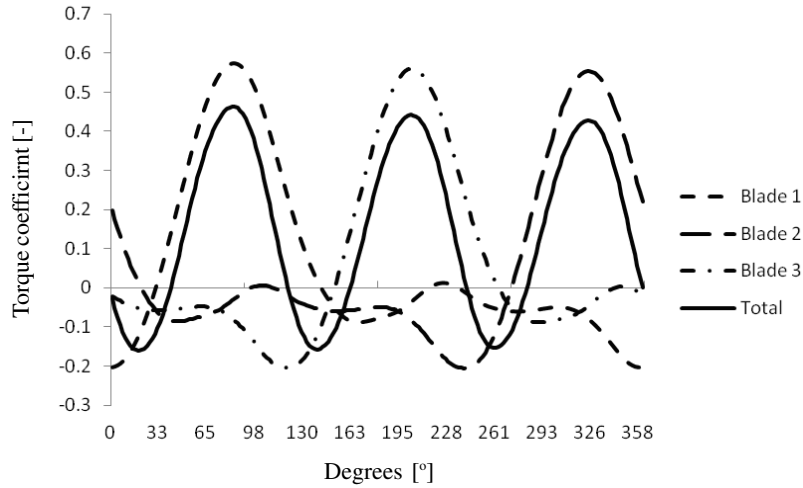
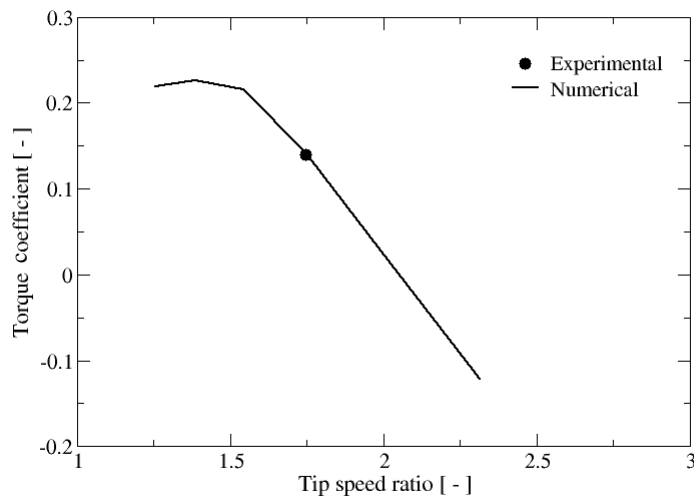
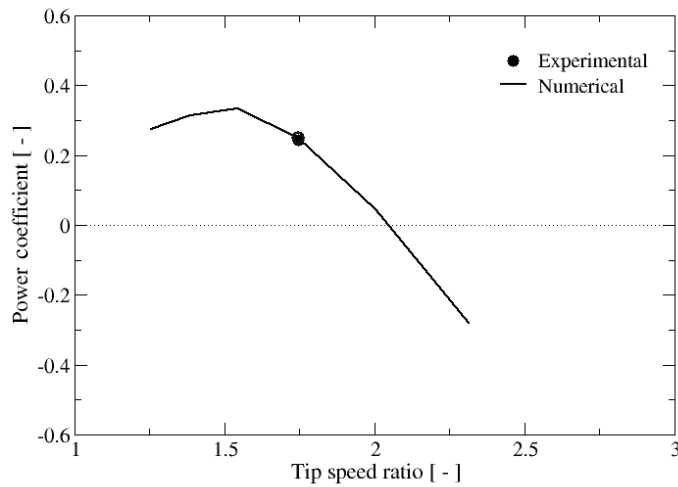


Fig. 6—Generation of torque coefficient by each blade in a revolution



a)



b)

Fig. 7—Tip speed ratio (λ) versus: a) Average torque coefficient; and b) Average power coefficient

around $\lambda = 1.35$ and decreases for lower values of λ because at low values of λ , flow around blades is separated, implying low lift and high drag. As a result, transferred torque from fluid to turbine decreases. Moreover, as C_p equals C_m times the λ , a behaviour of C_p similar to that of C_m is expected. Maximum C_p predicted by CFD is 33% at $\lambda = 1.6$ (Fig. 7b). Similar C_p curves are found in other CFWT^{6,11}. Unfortunately, Dai & Lam⁴ only provided data for a single point with $\lambda = 1.745$, instead of full $C_p(\lambda)$ curve (Fig. 7b).

Conclusions

A study of unsteady flow around a CFWT has been carried out using a transient rotor-stator approximation with a moving mesh technique in turbulent flow. Simulation results are in good agreement with experiments by Dai & Lam⁴ in a laboratory CFWT. Also, average torque and power coefficients versus tip speed ratio curves have been constructed for referred turbine. Overall, this work demonstrated that CFD model can effectively predict hydrodynamic performance of cross flow water turbines.

References

- 1 Laín S, *Modeling and Simulation of Bubble Induced Flows* (Universidad Autónoma de Occidente, Cali, Colombia) 2007 (In Spanish).
- 2 Laín S & Sommerfeld M, *Experimental and Numerical Study of the Motion of Non-Spherical Particles in Wall-Bounded Turbulent Flows* (Universidad Autónoma de Occidente, Cali, Colombia) 2008.
- 3 Laín S, *On Modeling and Numerical Computation of Industrial Disperse Two-Phase Flow with the Euler-Lagrange Approach* (Shaker Verlag, Aachen, Germany) 2010.
- 4 Ferreira C J S, *The near wake of the VAWT. 2D and 3D views of the VAWT aerodynamics*, PhD Thesis, Delt University of Technology, 2009.
- 5 Maître T, Achard J L, Guitet L & Ploesteanu C, Marine turbine development: numerical and experimental investigations, *Sci Bull Timisoara Politechnic Univ*, **50** (2005) 59-66.
- 6 Nabavi Y, *Numerical study of the duct shape effect on the performance of a ducted vertical axis tidal turbine*, M Sc Thesis, British Columbia University, 2008.
- 7 Dai Y M & Lam W, Numerical study of straight-bladed Darrieus-type tidal turbine, *ICE-Energy*, **162** (2009) 67-76.
- 8 Brochier G, Fraunie P, Beguier C & Paraschivoiu I, Water channel experiments of dynamic stall on Darrieus wind turbine blades, *J Propulsion & Power*, **2** (1986) 445-449.
- 9 Laín S, García M, Quintero B & Orrego, S, CFD numerical simulation of Francis turbines, *Rev Fac Ingeniería Univ Antioquia*, **51** (2010) 21-33.
- 10 Menter FR, Two-equation Eddy-viscosity turbulence models for engineering applications, *AIAA J*, **32** (1994) 269-289.
- 11 Coiro D P, De Marco A, Nicolosi F, Melone S & Montella F, Dynamic behaviour of the patented Kobold tidal current turbine: numerical and experimental aspects, *Acta Polytech Czech Tech Univ*, **45** (2005) 77-84.